

Available online at [www.sciencedirect.com](http://www.sciencedirect.com)

Procedia IUTAM 1 (2010) 64–73

---

---

**Procedia  
IUTAM**

---

---

[www.elsevier.com/locate/procedia](http://www.elsevier.com/locate/procedia)IUTAM Symposium on Computational Aero-Acoustics  
for Aircraft Noise PredictionReprint of: Parabolized stability equation models of large-scale jet mixing noise<sup>☆</sup>Tim Colonius<sup>a</sup>, Arnab Samanta<sup>a</sup>, Kristjan Gudmundsson<sup>a</sup><sup>a</sup>*Mechanical Engineering  
California Institute of Technology, Pasadena, CA 91125, USA*

---

**Abstract**

We report on the development of parabolized stability equation models to predict the evolution of low frequencies, large-scale wavepacket structures in turbulent jets and their radiated sound. We consider computations and data corresponding to high subsonic and supersonic jets from circular nozzles. Previous methods are extended to consider nonlinear interactions amongst the waves and use a Kirchhoff-surface type approach to project the near-field wavepacket amplitudes to the far-field. Linear PSE, whose initial conditions are chosen to provide an overall amplitude reference, show excellent agreement for the wavepacket amplitudes and phases with microphone array data just outside the jet shear layers, especially when the microphone data are processed to filter out contributions from uncorrelated fluctuations. Far-field sound predictions based on the linear PSE are also in reasonable agreement with far-field data. In order to investigate nonlinearity, we use an LES database to evaluate initial conditions for the PSE modes, and then compare their later evolution along the jet. Preliminary cases show some sensitivity to the initial amplitudes and their phases, and that nonlinear effects may be important in predicting the far-field sound based on the initial (near-nozzle) spectrum of disturbances.

© 2010 Published by Elsevier Ltd. Open access under [CC BY-NC-ND license](https://creativecommons.org/licenses/by-nc-nd/4.0/).*Keywords:* jet noise, parabolized stability equations, instability wave, turbulent jet

---

**1. Introduction**

Existing methods for prediction of turbulent jet noise are alternatively based on direct solution of the governing equations for a compressible flow, e.g. direct and large-eddy simulation (see [1]), or indirectly based on solution of an inhomogeneous wave equation (or other linearized equations [2]) together with specified statistical models for the equivalent sources of sound. The latter *acoustic analogy* approach is far less computationally intensive and has been pursued intensively since Lighthill's pioneering paper [3]. But despite recent advances (e.g. [4]), it is unclear that equivalent sources are universal or that they can be determined based solely on the mean jet flow field. These approaches would appear to be particularly fragile in cases where geometrical perturbations such as nozzle serrations or active control are considered. These noise suppression techniques generally produce modest sound reductions that are likely to be within the uncertainty inherent in the specification of statistical models of equivalent sources, especially when projected to the far field.

We are developing an alternative *direct* approach that is based on a coarse description of the large-scale turbulent structures, and a projection (or Kirchhoff surface approach) of near-field pressure signals associated with these structures to the far field. Large-scale structures in turbulent jets are associated with (inviscid) instabilities of the inflectional mean jet profile. Their large scale makes their evolution *relatively* insensitive to the finer-scale turbulence in the nozzle boundary layers, except through the impact of these scales on the jet mean flow field. If this is the case,

<sup>☆</sup> This article is a reprint of a previously published article. For citation purposes, please use the original publication details: *Procedia Engineering* 6C (2010) 64–73. DOI of original item: [10.1016/j.proeng.2010.09.008](https://doi.org/10.1016/j.proeng.2010.09.008)

and depending on the fidelity required, the disturbances could, in principle, be predicted by solving for disturbances to the jet mean flow field, which in turn might be rapidly predicted via Reynolds Averaged Navier-Stokes (RANS) equations. The approach of considering direct sound radiation from instabilities of turbulent shear layers has been considered in the past [5, 6, 7, 8]. Except for forced, supersonic jets, where near-field fluctuations were found to be in good agreement with predictions of linear stability theory [9], these previous efforts have not resulted in quantitative predictions of sound generation in natural (unforced) jets.

In our earlier work [10], we in fact showed that the pressure fluctuations measured *just outside the jet shear layers* were consistent with the evolution inferred from modeling them as *linear* instability waves computed by a locally parallel flow analysis of the jet mean flow field, provided that a suitable frequency-dependent number is chosen for amplitude near the nozzle exit. More generally, a weakly non-parallel analysis [11, 12] or a global mode analysis [13] could provide the description of the fluctuations. In what follows, we refer to the disturbances as wave packets (or instability waves), regardless of the particular methodology used to describe their evolution. The name is based on the wave-packet structure of the pressure field evident in experimental data and numerical simulations. In this paper, we show that a Parabolized Stability Equation (PSE) approach [14] provides a reasonable compromise between fidelity and rapid computation for prediction of the wave packets.

Because of ambiguity inherent to a linear approach, these analyses have not yet demonstrated that the representation of the structures as *linear* disturbances is sufficient and consistent with the actual measured disturbance spectrum in the near-nozzle region. Indeed, there is some evidence [15] that nonlinear interactions play a significant role in determining the wavepacket evolution. If nonlinear interactions are important, PSE may be generalized to consider nonlinear interactions amongst the modes. Further discussion of this point and preliminary results of nonlinear analysis are discussed later in the paper.

Evidence suggests that the wave-packet structures which dominate the near pressure field are sufficiently acoustically efficient so as to also represent a significant portion of the far-field sound [16]. Thus our premise, supported by previous work and the analysis presented below, is that if the near pressure field associated with the large scales can be predicted accurately enough, then prediction of the far-field sound will follow directly by a Kirchhoff surface strategy. Further support for this stance follows from prevailing theories and data that show that the highly directive aft-angle radiation is dominated by disturbances associated with the large scales [17].

To summarize, we argue for direct noise prediction strategy that is based on a coarse description of the large-scale turbulent structures, which is in turn based on linear or nonlinear PSE together with a RANS-based mean flow prediction, and an extrapolation of the pressure field from just outside the shear layer to the far field. To be fully predictive, of course, we must also have knowledge of the near nozzle spectrum of disturbances that provide initial conditions for the PSE computation. This is a difficult challenge that has not yet been met, but even in the absence of a definitive initial spectrum much can be learned about the sensitivity (or lack thereof) of the far-field sound to the near-nozzle disturbance amplitudes. An advantage of the model is that it provides a direct assessment of the sound emitted by the large-scale structures which are, in turn, the feature of the jet flow field that is most amenable to control by perturbation of the near nozzle flow field.

The remainder of this paper provides some details on the individual components that comprise the model, as well as validation of the modeling with data from experiments and large eddy simulations. In the next section, we briefly describe the PSE formulation. Results based on linear PSE are then compared to raw microphone data in both near and far-fields. Next, we present preliminary results obtained using nonlinear PSE to describe the wave packet evolution.

## 2. PSE Formulation

Parabolized stability equations [18, 14, 19, 20, 21, 22, 23, 11] represent an *ad hoc* but powerful generalization of parallel-flow linear stability analysis for convectively unstable flows. In our version of PSE, we decompose the flow into a mean (time-average) component and its fluctuations:

$$q = \bar{q} + q'$$

where  $q = [u_x \ u_r \ u_\theta \ T \ \rho]^T$ . The mean flow,  $\bar{q}$  is given either from a RANS model or from experimental data (PIV). In the PSE Ansatz, the fluctuations are further written as

$$q'(x, r, \theta, t) = \sum_{n=-N}^N \sum_{m=-M}^M \bar{q}_{mn}(x, r) \exp(i(m\theta - n\omega t)),$$

where  $\bar{q}_{mn}$  is then decomposed into a slowly varying shape function and a rapidly varying wave-like part:

$$\bar{q}_{mn}(x, r) = \hat{q}_{mn}(x, r) \hat{\alpha}_{mn}(x) = \hat{q}_{mn}(x, r) \exp\left(i \int^x \alpha_{mn}(\xi) d\xi\right), \quad (1)$$

where  $\alpha_{mn}$  and  $\hat{q}_{mn}$  upon numerical discretization will be represented with a coarse spatial increment,  $\Delta x$ . The real and imaginary parts of  $\alpha_{mn}$  represent the axial wavenumber and growth rate, respectively. Here  $m$  is the azimuthal wavenumber and  $\omega$  is the angular frequency. The modes are truncated to some finite number  $M$  and  $N$ , respectively. This expression is substituted into the full compressible Navier-Stokes, energy, and continuity equations, resulting in the following system of equations:

$$(\mathbf{A}(\bar{\mathbf{q}}, \alpha, m, \omega) + \mathbf{B}(\bar{\mathbf{q}})) \hat{\mathbf{q}} + \mathbf{C}(\bar{\mathbf{q}}) \frac{\partial \hat{\mathbf{q}}}{\partial x} + \mathbf{D}(\bar{\mathbf{q}}) \frac{\partial \hat{\mathbf{q}}}{\partial r} = \frac{1}{\text{Re}} \mathbf{E}(\bar{\mathbf{q}}) \hat{\mathbf{q}} + \frac{\hat{\mathbf{F}}_{mn}(x, r)}{\hat{\alpha}_{mn}}. \quad (2)$$

For brevity, the linear operators  $\mathbf{A}$  to  $\mathbf{E}$  are not written out, we refer the reader to ref [24] for details. All nonlinear terms are lumped into  $\hat{\mathbf{F}}_{mn}$ , and, when present, this term is evaluated using a pseudo-spectral approach using a Fourier transform and performing nonlinear multiplications in physical space.

Under the slowly varying approximation, the viscous terms are simplified by only retaining terms involving derivatives in the radial direction (thin shear layer approximation).

The decomposition of (1) is ambiguous in that the streamwise development of  $\bar{q}$  can be absorbed into either the shape-function  $\hat{q}$  or in the wavenumber/growth-rate function  $\hat{\alpha}$ . Following Herbert [14], we use a normalization condition on the shape function

$$\int_0^\infty \hat{\mathbf{q}} \frac{\partial \hat{\mathbf{q}}^*}{\partial x} r \, dr = 0, \quad (3)$$

which removes any exponential dependence on the shape function  $\hat{\mathbf{q}}$ .

We discretize equations (2) using fourth-order central differences in the radial direction, closing the domain with the characteristic boundary conditions of Thompson [25]. The streamwise derivative is approximated via first-order implicit Euler differences, and this results in a system of equations to solve for the shape functions at each position on the jet axis. When nonlinear terms are retained, the equations must be solved iteratively. Parabolization implies some restrictions on the step size,  $\Delta x$ , which are discussed in [24]. The wavenumber is also updated on each step by solving [21]

$$\alpha_{j+1}^{n+1} = \alpha_{j+1}^n - \frac{i}{\Delta x} \frac{\int_0^\infty (\hat{\mathbf{q}}_{j+1}^n)^* (\hat{\mathbf{q}}_{j+1}^n - \hat{\mathbf{q}}_j^n) r \, dr}{\int_0^\infty |\hat{\mathbf{q}}_{j+1}^n|^2 r \, dr}, \quad (4)$$

where  $n$  is the iteration step index.

Initial conditions  $(\hat{q}_{mn}, \alpha_{mn})_{x_0}$  for (2) are obtained by solving a parallel flow stability problem for the velocity profile at the initial position (which is typically just downstream from the nozzle lip). The initial stability problem is solved by a standard shooting approach [24].

The nonlinear forcing term provides a nonzero contribution at zero frequency, zero azimuthal wavenumber. Some investigators have used this term to solve an additional “mean flow correction” to the specified initial base flow. This approach has the merit of consistency and can provide reasonable predictions for low Reynolds number, transitional shear layers [26]. However, for model and full-scale jets, we do not expect the Reynolds stresses associated with the limited large-scale PSE description to provide the full Reynolds stresses that would be consistent with the measured or RANS-computed mean flow field used in our decomposition. We therefore discard any mean flow correction in our approach. However, we note that the nonlinear contribution to the mean flow from the fluctuations may in fact provide useful additional data that could be used in future to supplement the PSE formulation with a turbulence model that would attempt to account for the unresolved scales of turbulence.

### 3. Linear PSE and microphone array data

In this section and the next one, we study two  $M_\infty = U_j/a_\infty = 0.9$  jets, one unheated and one with  $T_j/T_\infty = 2.7$  (and  $M_j = 0.56$ ), and a single unheated supersonic jet with  $M_j = 1.5$ . The subsonic jets both used a 2 inch converging nozzle and mean flows were measured using stereoscopic PIV in the SHJAR facility at NASA Glenn Research Center [27, 28]. The supersonic jets were measured at the ART facility at United Technologies Research Center using a CD (method-of-characteristics) nozzle with a 3 inch exit diameter that was close to perfectly expanded [29]. For this flow, we used a mean flow predicted using RANS, computed by Cascade Technologies [30], using the same nozzle specifications as the experiment. Further details regarding the mean flows may be found in the references.

We compare the PSE results to pressure fluctuations measured by microphone arrays placed just outside the jet shear layer. For the subsonic jets, the Glenn microphone array consisted of 13 concentric rings of 6 microphones on a conically expanding surface (cone angle  $11.2^\circ$ ). Near the nozzle lip, the first ring had a diameter of  $1.75D$ , and this increased to  $4.75D$  just after  $x/D = 8$ . The 78 microphones recorded the pressure simultaneously.

For the supersonic jets, measurements were conducted at the ART facility using a novel rotating array [29] which consisted of two linear microphone arrays, with one fixed and the other rotated automatically in the azimuthal direction. The second array (i.e. the reference array) is also movable, but requires manual adjustment. For a given position of the reference array, phase-locked data between the two arrays is acquired for each location. With this approach, the modal content at any axial location is determined by Fourier transformation of the two-point azimuthal correlation. For the results reported here, 8 microphones were used on each linear array, encompassing approximately  $10D$ . Microphones were spaced axially by  $1.25D$ , with a spreading angle (cone half-angle) of  $\pm 7$  degrees. The first microphone was located at  $1.13D$  from the nozzle exit, at a radial distance of  $0.97D$  from the jet centerline. The downstream-most microphone was located at  $9.88D$ , at a radial distance of  $2.05D$ .

It should be noted that the microphone arrays were carefully positioned to attempt to place them in a location near enough to the shear layer such that the signal would be predominantly hydrodynamic (convective), but sufficiently far so that fluctuation levels were very low and one may assume that they are linear (such that we can project the data to the acoustic far-field with as little ambiguity as possible). In practice, and depending on the specific conditions, there are uncorrelated acoustic waves arising from other sources of sound (e.g. finer scale turbulence) that are also measured by the arrays. We discuss this issue further below.

Due to space limitations in this paper, we present results which are representative of a much more extensive set of comparisons. These further comparisons are available in [24]. The conclusions demonstrated here apply broadly across the conditions we have considered.

We begin by looking at linear PSE, where we set  $\hat{\mathbf{F}}_{mn} = 0$ . In figure 1 we compare PSE to experimental data for the  $M_\infty = 0.9$  unheated jet. Because linear fluctuations are independent of the overall amplitude and phase of each mode (frequency and azimuthal wavenumber), we take the liberty of adjusting each mode by a single complex number to obtain the best fit at the array's microphone locations. In this way we are only assessing the shapes and relative phases of each mode as compared to the PSE predictions. This issue is discussed further in the context of nonlinear results in section 4.

Overall the raw microphone data (open circles) are in reasonable agreement with the linear evolution from PSE. With the exception of the lowest frequency, axisymmetric mode, the early evolution up to about  $x/D = 4$  is in very good agreement. For  $x/D > 4$ , the microphone data is more energetic than the PSE. To better assess this discrepancy, we applied a statistical technique called the proper orthogonal decomposition (POD) to the microphone data. For each azimuthal mode, the cross-spectral matrix of the 13 microphone rings is found and the eigenvector corresponding to its greatest eigenvalue is retained and plotted as the open squares in the figure. This technique should suppress parts of the microphone signal that are uncorrelated with the dominant portion of the signal, such as acoustic waves that might arise from uncorrelated sources (or other pressure fluctuations from finer scale turbulence). Indeed, the linear PSE evolution displays a remarkable agreement with the first POD mode of the microphone data. This agreement extends to the phase of the wave packets, as demonstrated in figure 2.

The POD slightly cleans up the agreement for the lowest frequency  $m = 0$  mode, but this mode remains more poorly predicted by PSE. We note that at other conditions (particularly at lower  $M$ ), we obtain a better representation of the lowest frequency mode [24]. The discrepancy for this mode may be related to nonlinear effects discuss in the next section.

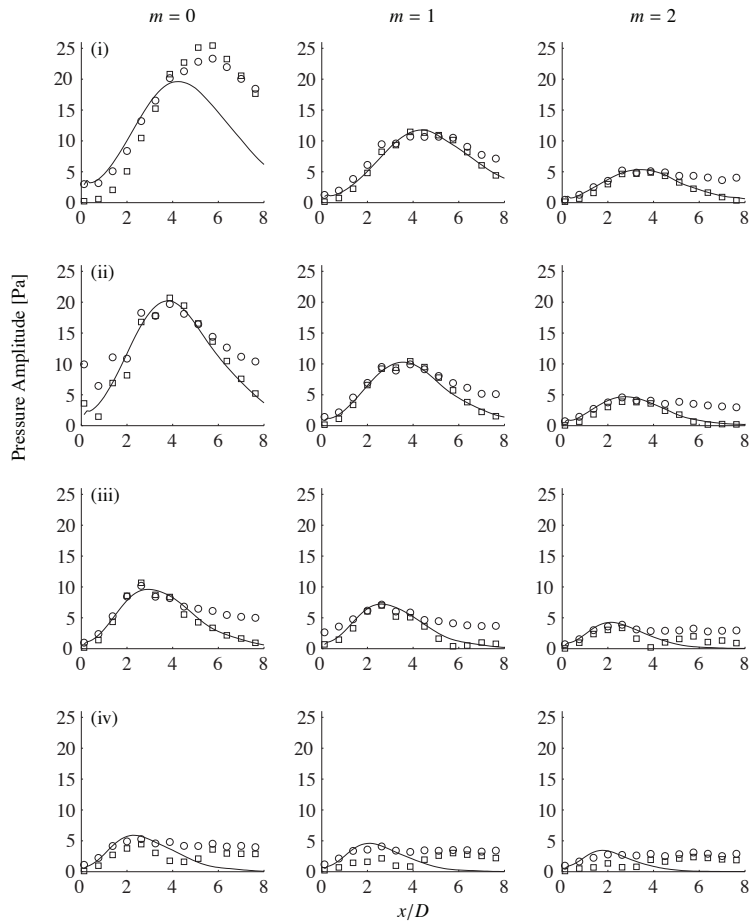


Figure 1: Pressure amplitude along the microphone array for the cold  $M_j = 0.9$  jet: (○) microphone data; (□) first POD-mode of cross-spectral matrix; (—) PSE-predictions, all at frequencies (i)  $St = 0.25$ ; (ii)  $St = 0.35$ ; (iii)  $St = 0.5$ ; (iv)  $St = 0.65$ .

We now turn to the far-field sound associated with the wavepackets. In Reba et al. [16], wavepackets as directly measured along the NASA near-field array were projected to the acoustic far field using a Kirchhoff surface methodology. Due to the limited streamwise extent of the microphone array measurements, the predictions were based on curve-fits to the two-point pressure correlations measured along the array, and then extrapolated to greater distances downstream based on an assumed Gaussian-type model for the wave packet. It was shown that the far-field pressure was reasonably well predicted at aft angles, and over a range of low frequencies and operating conditions, by the modeled correlation functions. This provided direct evidence that large-scale wave-like structures dominated the aft radiation at high subsonic speeds (jets with  $M_j = 0.9$  and temperature ratios of 1.76 and 2.7 were considered).

Here we use this methodology to project the PSE-predicted, linear wave packets to the far field. In figure 3 (left 4 panels), the pressure autocorrelation is plotted at positions along the microphone array are shown for 4 low

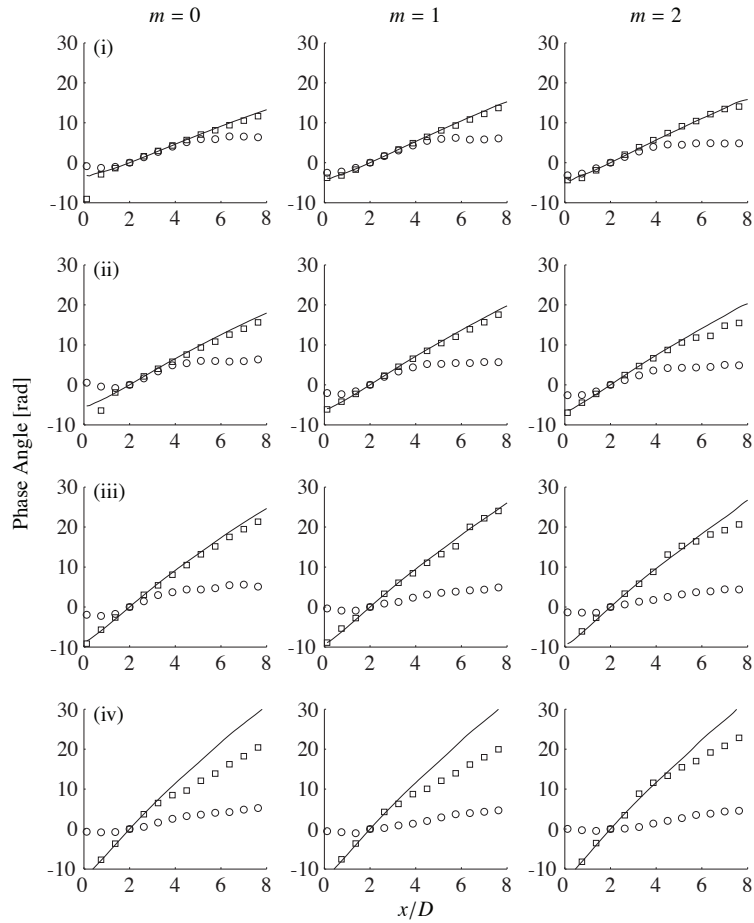


Figure 2: Phase-angle along the microphone array for the cold  $M_j = 0.9$  jet: (○) ensemble-average; (□) first POD-mode; (—) PSE-predictions, at frequencies (i)  $St = 0.25$ ; (ii)  $St = 0.35$ ; (iii)  $St = 0.5$ ; (iv)  $St = 0.65$ .

frequencies and for  $m = 0$ , for the  $M_\infty = 0.9$ , heated ( $T_j/T_\infty = 2.7$ ) jet. Superposed on the experimental data (from the near field array) is the Gaussian wave-packet model of Reba et al. [16] as well as the PSE predicted evolution, where the amplitude has been set in each case to give the best agreement with the microphone data over the first 6 to 8 jet diameters. Despite the (surprisingly large) discrepancy between PSE and the assumed (and extrapolated) form of the correlations, the right panels of figure 3 show that the far acoustic field at aft angles is reasonably well predicted by both the model and the PSE. The more compact, lower amplitude shape of the PSE correlation, in general, results in lower sound, but the peak radiation at aft angles is within a few dB of the data. Neither model nor PSE performs well at angles closer to sideline, but this is expected since small scale turbulence contributes a large portion of the radiation observed at those angles. Overall, the comparison is encouraging and demonstrates the feasibility of using PSE to directly predict acoustic radiation of large structure noise in the jet.

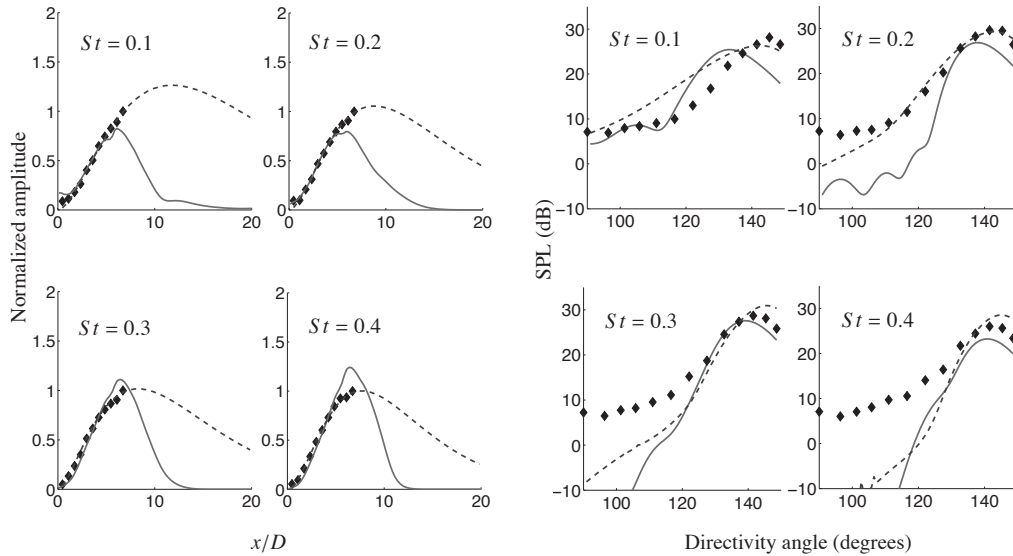


Figure 3: Left: Pressure correlation along microphone array. Right: Far-field projection. (◆) near-field and far-field microphone data, respectively; (—) PSE solution; (---) Gaussian model of [16]. For  $M_j = 0.9$ ,  $T_j/T_\infty = 2.7$ ,  $m = 0$ .

#### 4. Nonlinear PSE

In this section we provide a preliminary overview of the non-linear implementation of our PSE method (NPSE). Non-linear effects are likely to be important for the lower-order modes, particularly near and beyond the closing of the jet potential core where the wave amplitudes have obtained their maximum values. One critical aspect of the NPSE method is the requirement to provide a correct estimate of the near-nozzle disturbance spectrum as the initial condition. Linear solutions do not require this and their evolution is independent of the initial amplitude. In principle, experimental data or high-fidelity simulations could provide such data; the hope is that there is some measure of universality in the initial spectra, or that initial amplitudes can at least be systematically varied in order to determine the bounds on the resulting noise radiation.

As we do not have experimental data for matching conditions as the microphone arrays, we turn to an LES simulation [30] of the same  $M_j = 1.5$  jet discussed in the previous section to provide the initial conditions for the purposes of model development and validation. The LES data include both near and far-field pressure fluctuations, which we use for comparison with NPSE. We also used the LES to provide the mean flow for the NPSE. It is also noted that the LES computations included the solid geometry of the nozzle, which imitated the experimental CD nozzle of Schlinker et al. [29].

Before discussing the results, we provide a brief discussion of the validation of the NPSE code that we developed. NPSE provides further challenges in that it is not known *a priori* how many modes need to be retained and what is the sensitivity to the initial amplitudes. Often times, the marching algorithm (parabolization) fails to converge when nonlinear interactions become significant [26]. To validate our implementation, we first compared our results for a two-dimensional, planar shear layer that was considered by Day [26] and is based on a low Reynolds number DNS of the same flow [31]. The growth rates of the fundamental and first two subharmonic frequencies were examined in detail (results are not presented here for brevity), and showed excellent agreement with the previous NPSE and the DNS. We note that in this case, we retained the mean-flow correction discussed in section 2.

Next, we used the NPSE to simulate a recently proposed nonlinear wave interaction model [15]. This study

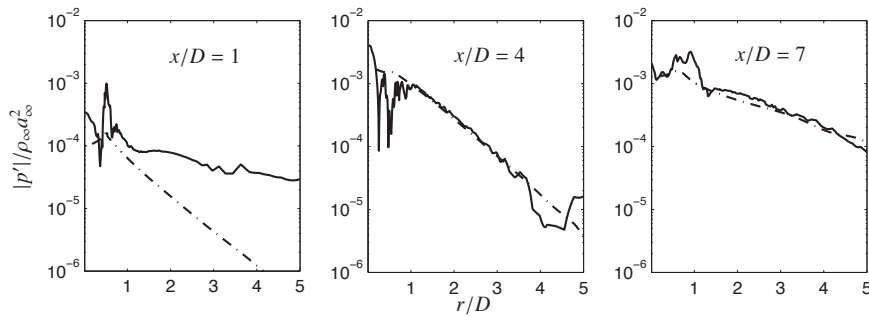


Figure 4: Comparison of radial profiles of LES fluctuations (—) with nonlinear PSE (---) predictions for  $M_j = 1.5$  jet at  $St = 0.3$ ,  $m = 0$ . The initial amplitudes at  $x/D = 1$  were set to obtain the best visual agreement of the profiles and amplitudes at  $x/D = 4$ .

stressed the importance of interactions between instability mode pairs and how the resulting “difference-frequency” mode is expected to dominate far-field radiation. Our present interest is simply confined to reproducing some of the near-field non-linear interaction results, which were obtained using a DNS approach. An analytical base flow is used as described in the reference [15] and not repeated here. Input disturbances come from LST solutions, where the amplitudes  $A$  of the dominant mode pair at the inlet, is chosen from the reference [15]. We consider two cases corresponding to cases A2 and A3 of Suponitsky et al. In these cases, axisymmetric modes,  $m = 0$ , were initialized at  $St = 0.3$  and  $0.5$ . The two cases consisted of initializing these modes at low amplitude and examining the energy transfer to the difference mode at  $St = 0.2$ . We compared the pressure magnitudes at different streamwise positions at  $r/D = 0.7$  to the data reported by Suponitsky et. al., and found good agreement with the predicted amplitudes of the nonlinearly generated difference mode at  $St = 0.2$ .

Returning now to the  $M_j = 1.5$  cold jet, the first task is to match the modal amplitudes near the nozzle exit to provide initial conditions for NPSE. In reality, LES fluctuations involve a much wider range of scales than can be represented in a PSE Ansatz. To provide the best representation of the NPSE near-nozzle input fluctuations, these uncorrelated components need to be filtered out via techniques like the Proper Orthogonal Decomposition (POD). In the present paper, instead, the LES data is simply time-Fourier-transformed while retaining the phase information. This is important, since the non-linear interactions depend on the initial phases as well as amplitudes. For NPSE, the initial modal profiles are obtained via Linear Stability (LST) solutions, but their amplitudes are adjusted by fitting the NPSE with the LES radial profiles at some streamwise locations close to the nozzle exit. This is an iterative procedure, where the method is designed to obtain the “best” visual match between  $x/D = 1$  and  $x/D = 4$ . The position  $x/D = 1$  was chosen to avoid the expected “numerical transition” of the LES data closer to the nozzle, which may render the turbulent fluctuations upstream of this point unrealistic.

Figure 4 shows the radial evolution of the  $M_j = 1.5$  cold jet for one of its modes ( $St = 0.3$ ,  $m = 0$ ) at some streamwise locations obtained by the aforementioned iterative procedure for determining the initial amplitudes. By  $x/D = 4$ , a reasonable quantitative agreement of modal shapes emerges between LES and NPSE, despite the relatively crude representation at  $x/D = 1$ . Obviously the LES data is richer and includes contributions beyond what NPSE can capture. Similarly, it should be cautioned that a relatively short period of LES data (about 100 convective units) was used in performing the Fourier transforms, and there is a significant amount of statistical scatter for the low frequencies.

The NPSE simulations were performed by retaining 15 modes (5 frequencies from 0.1 to 0.5 and azimuthal modes  $m = 0, 1, 2$ ). In general, we have observed that retaining more modes typically results in better agreement, but owing to the incomplete parabolization of the PSE equations there is a restriction on the minimum marching step size associated with the highest frequency, that can be destabilizing for lower order modes[21]. The range of frequencies we retained in this calculation balanced the competing demands, but, nevertheless, we could only obtain converged results up to  $x/D = 7.5$  for this case. Further study will be required to sort out these convergence issues.

Figure 5 shows the streamwise evolution of pressure fluctuation amplitudes for selected modes. Two different



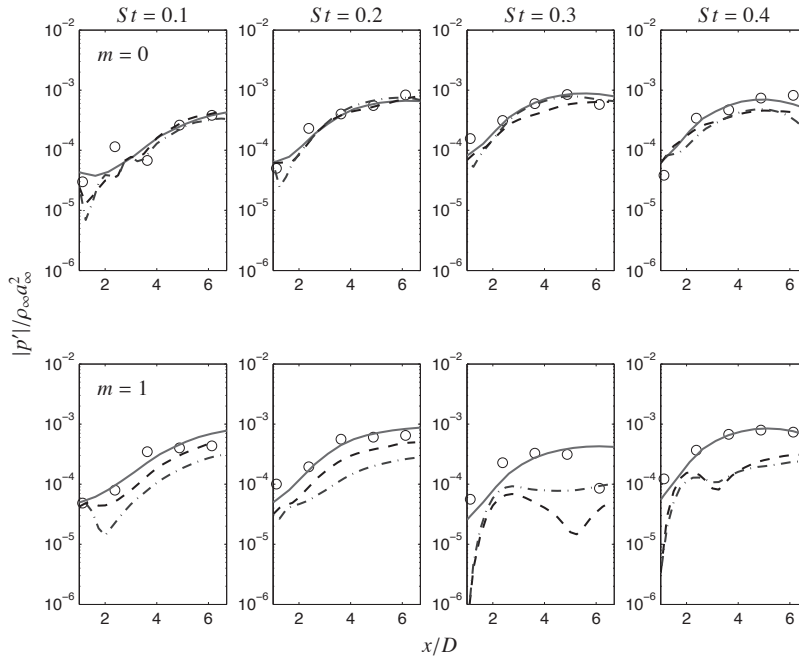


Figure 5: Evolution of pressure amplitude of all frequencies and wavenumbers along the UTRC microphone array. LES data ( $\circ$ ) is compared to linear PSE (—), NPSE with different phases to the modes at the inlet (---), and another NPSE with zero phase (-.-).  $M_j = 1.5$ .

NPSE runs are shown; they differed in that in one case the initial phases were taken from the LES signals, whereas in the second case, all modes were initiated at the same phase. Linear PSE runs which selected initial amplitudes that gave the best overall agreement with the LES data are also presented. The NPSE solutions generally appear to be in reasonable agreement with the LES data for lower frequencies and for the axisymmetric mode. Although the linear PSE does as well or better, note that the initial amplitudes at  $x/D = 1$  are very different, especially for some of the higher modes. This indicates the importance of non-linearity in the solutions, and potential problems with specifying an initial disturbance amplitude solely on the basis of an assumed linear evolution. Nonlinearity is also evident in the differences between the two NPSE cases with different initial phases, especially for those modes that do not agree well with the LES data, and so an “appropriate” choice of phase could potentially improve the NPSE predictions.

Clearly the results in this section are but a first step in a more systematic study to follow. However, we can conclude that some effects of nonlinearity are evident in the  $M_j = 1.5$  wavepacket evolution. Relatively good agreement for some of the modes in the NPSE solutions (and the good comparison with full DNS results of ref [15]), however, provides some optimism that rapid NPSE predictions may yield acceptable predictions for the wave packet amplitude, and, based on the results of the previous section, its extension to the far field.

#### Acknowledgements

This work was supported by NAVAIR through an SBIR contract to TTC Technologies, Inc., and through an STTR contract to CASCADE Technologies, Inc. The technical monitor was Dr. John Spyropoulos. We would like to thank the TTC and CASCADE teams for their collaboration and for sharing data presented in this paper. The authors would

like to specially thank Drs. Robert Schlinker and Ramons Reba of United Technologies Research Center for their extensive help and collaborations over many years, and for the experimental data used in this paper.

- [1] T. Colonius, S. Lele, Computational aeroacoustics: progress on nonlinear problems of sound generation, *Prog. Aerospace Sci.* 40 (2004) 345–416.
- [2] M. Goldstein, A generalized acoustic analogy, *J. Fluid Mech.* 488 (2003) 315–333.
- [3] M. Lighthill, On sound generated aerodynamically. I. General theory, *Proc. R. Soc. Lond. A* 211 (1107) (1952) 564–587.
- [4] S. Karabasov, M. Afsar, T. Hynes, A. Dowling, W. McCullan, C. Pokora, G. Page, J. McGuirk, Using large eddy simulation within an acoustic analogy approach for jet noise modelling, *AIAA Paper 2008-2985*.
- [5] E. Mollo-Christensen, Jet noise and shear flow instability seen from an experimenter's viewpoint, *J. Applied Mech.* 34 (1967) 1–7.
- [6] J. T. C. Liu, Developing large-scale wavelike eddies and the near jet noise field, *J. Fluid Mech.* 62 (1974) 437–464.
- [7] R. Mankbadi, J. T. C. Liu, A study of the interactions between large-scale coherent structures and fine-grained turbulence in a round jet, *Proc. Roy. Soc. London* 1443 (1981) 541–602.
- [8] P. Morris, M. Giridharan, G. Lilley, On the turbulent mixing of compressible free shear layers, *Proc. R. Soc. Lond. A* 431 (1990) 219–243.
- [9] C. Tam, P. Morris, Tone excited jets – Part V: A theoretical model and comparison with experiments, *J. Sound Vib.* 102 (1985) 119–151.
- [10] T. Suzuki, T. Colonius, Instability waves in a subsonic round jet detected using a near-field phased microphone array, *J. Fluid Mech.* 565 (2006) 197–226.
- [11] K. Gudmundsson, T. Colonius, Parabolized stability equation models for turbulent jets and their radiated sound, *AIAA Paper 2009-3380*.
- [12] N. Sandham, A. Salgado, Nonlinear interaction model of subsonic jet noise, *Phil. Trans. Roy. Soc. A* 366 (2008) 2745–2760.
- [13] J. Nichols, S. Lele, P. Moin, Global mode decomposition of supersonic jet noise, in: *Center for Turbulence Research Annual Research Briefs*, Stanford, CA, 2009.
- [14] T. Herbert, Parabolized stability equations, *Annu. Rev. Fluid Mech.* 29 (1997) 245–283.
- [15] V. Suponitsky, N. Sandham, C. Morfey, Linear and nonlinear mechanisms of sound radiation by instability waves in subsonic jets, Submitted to *J. Fluid Mech.*
- [16] R. Reba, S. Narayanan, T. Colonius, Wave-packet models for large-scale mixing noise, accepted for publication, *Int. J. Aeroacoustics*.
- [17] C. Tam, Supersonic jet noise, *Annu. Rev. Fluid Mech.* 27 (1) (1995) 17–43.
- [18] F. P. Bertolotti, T. Herbert, Analysis of the linear stability of compressible boundary layers using the PSE, *Theoret. Comput. Fluid Dyn.* 3 (1991) 117–124.
- [19] M. R. Malik, C. L. Chang, PSE applied to supersonic jet instability, *AIAA Paper 1997-0758*.
- [20] M. R. Malik, C. L. Chang, Nonparallel and nonlinear stability of supersonic jet flow, *Computers and Fluids* 29 (2000) 327–365.
- [21] M. Day, N. Mansour, W. Reynolds, Nonlinear stability and structure of compressible reacting mixing layers, *J. Fluid Mech.* 446 (2001) 375–408.
- [22] P. Ray, L. Cheung, S. Lele, On the growth and propagation of linear instability waves in compressible turbulent jets, *Physics of Fluids* 21 (2009) 054106.
- [23] L. Cheung, S. Lele, Linear and nonlinear processes in two-dimensional mixing layer dynamics and sound radiation, *J. Fluid Mech.* 625 (2009) 321–351.
- [24] K. Gudmundsson, Instability wave models of turbulent jets from round and serrated nozzles, Ph.D. thesis, California Institute of Technology (2010).
- [25] K. Thompson, Time dependent boundary conditions for hyperbolic systems, *J. Comp. Phys.* 68 (1987) 1–24.
- [26] M. J. Day, Structure and stability of compressible reacting mixing layers, Ph.D. thesis, Stanford University (1999).
- [27] J. Bridges, M. Wernet, Measurements of the aeroacoustic sound source in hot jets, *AIAA Paper 2003-3130*.
- [28] J. Bridges, C. A. Brown, Parametric testing of chevrons on single flow hot jets, *AIAA Paper 2004-2824*.
- [29] R. Schlinker, R. Reba, J. Simonich, T. Colonius, K. Gudmundsson, F. Ladeinde, Towards prediction and control of large-scale turbulent structure supersonic jet noise, *Proceedings of ASME Turbo Expo 2009 (GT2009-60301)*.
- [30] Y. Khalighi, F. Ham, P. Moin, S. Lele, T. Colonius, R. Schlinker, R. Reba, Unstructured large eddy simulation technology for prediction and control of jet noise, *Proceedings of the ASME Turbo Expo 2010 (GT2010-22306)*.
- [31] T. Colonius, S. K. Lele, P. Moin, Sound generation in a mixing layer, *J. Fluid Mech.* 330 (1997) 375–409.